Supplemental Information

Experimental Section

Materials: 3-aminopropyl-(hepta-isobutyl) POSS (AMPO) was purchased from Hybrid plastic. 3,5-dinitrobenzoyl chloride (99%), 6-maleimidohexanoic acid (98%), ethyl 2-ethoxyquinoline-1(2H)-carboxylate (EEDQ, 99%), triethylamine (Et_3N, 99%), acetyl chloride (99%), m-phenylenediamine (99%) and palladium/carbon (10%) (50% wet with water for safety) were purchased from Alfa. Polytetramethylene ether glycol (PTMEG, Mn= ~1000 g mol^{-1}), isophorone diisocyanate (IPDI, 99%) and 2,5-furandimethanol (FDO, 98%) were purchased from Aladdin. Anhydrous tetrahydrofuran (THF, 99.5%), anhydrous acetonitrile (99.9%), anhydrous 1,4-dioxane (99.5%), dichloromethane (99.9%) and methanol (99.9%) were purchased from Adamas. All reagents were used as received without further purification unless otherwise noted.

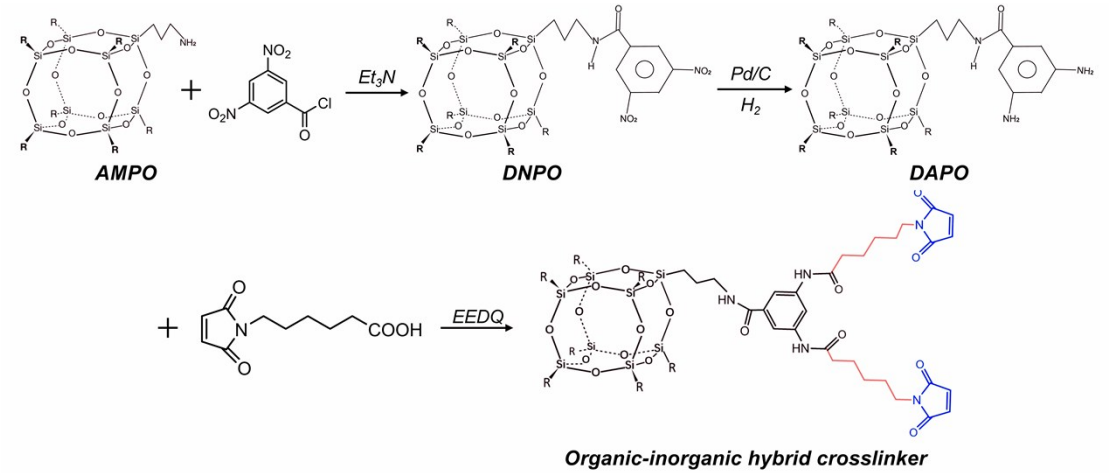

Scheme S1. Schematic representation of synthesis of organic-inorganic hybrid crosslinker.

Synthesis of N-[(Hepta-isobutyl-POSS) propyl]-3, 5-dinitrobenzamide (DNPO): A THF solution (20 mL) with 3,5-dinitrobenzoyl chloride (2.7g, 11.67 mmol) was slowly added into a THF solution (100 mL) with 3-aminopropyl-(hepta-isobutyl) POSS (AMPO) (9.72g, 11.12 mmol) and triethylamine (1.5 mL) at 0 °C. The mixture was stirred at 0 °C for 1h, and then was stirred at 25 °C for 5h. After filtrating, the filtrate was evaporated to remove the solution, obtaining an off-white solid. The white solid was dissolved into CH_2Cl_2, and the solution was washed with water, and then dried over Na_2SO_4. After evaporating the solvent under reduced pressure, pure DNPO (11.71 g, yield 98%) was obtained as a white solid. ^1H NMR ($CDCl_3$, 400 MHz, ppm, see Fig. S1a): δ= 9.17 (t, 1H, -$C_6\underline{H}_3$), 8.93 (d, 2H, -$C_6\underline{H}_3$), 6.30 (s, 1H, -N$\underline{H}$-CO-), 3.51-3.56 (m, 2H, -$C\underline{H}_2$-NHCO-), 1.80-1.91 (m, 7H, -CH_2-$C\underline{H}$-$(CH_3)_2$), 1.73-1.78 (m, 2H, -$C\underline{H}_2$-CH_2-NHCO-), 0.93-0.97 (d, 42H, - CH_2-CH-($C\underline{H}_3)_2$), 0.67-0.72 (t, 2H, -$C\underline{H}_2$-CH_2-CH_2-NHCO-), 0.58-0.63 (m, 14H, -$C\underline{H}_2$-CH-$(CH_3)_2$); ^{13}C NMR ($CDCl_3$, 400 MHz, ppm, see Fig. S1b): δ= 162.59, 148.67, 138.22, 127.02, 120.99, 43.05, 25.67, 22.93, 22.46, 22.44, 9.63.

Synthesis of N-[(Hepta-isobutyl-POSS) propyl]-3, 5-diaminobenzamide (DAPO): DNPO (11.71 g, 10.97mmol), Pd/C (loading of Pd is 10%), THF (100 mL) and methanol (50mL) were added

into a Schlenk flask which was charged with hydrogen (~2 psig, then 4 evacuation/backfill cycles). The mixture was stirred for 24 h at 25 °C, and then was filtrated through a pad of Celite to obtain clear solvents. After evaporating the solvent under reduced pressure, DAPO as an off-white solid (10.55 g, yield 95%) was obtained. ^{1}H NMR ($CDCl_3$, 400 MHz, ppm, see Fig. S2a): δ= 6.45 (d, 2H, -$C_6\underline{H}_3$), 6.12 (s, 1H, -$C_6\underline{H}_3$), 5.98 (s, 1H, -N<u>H</u>-CO-), 3.37-3.42 (m, 2H, -C<u>H</u>$_2$-NHCO-), 1.80-1.85 (m, 7H, -CH_2-C<u>H</u>-$(CH_3)_2$), 1.63-1.71 (m, 2H, -C<u>H</u>$_2$-CH_2-NHCO-), 0.94-0.96 (d, 42H, - CH_2-CH-(C<u>H</u>$_3$)$_2$), 0.62-0.63 (t, 2H, -C<u>H</u>$_2$-CH_2-CH_2-NHCO-), 0.59-0.61 (m, 14H, -C<u>H</u>$_2$-CH-$(CH_3)_2$); ^{13}C NMR ($CDCl_3$, 400 MHz, ppm, see Fig. S2b): δ= 167.80, 147.48, 137.30, 104.19, 103.86, 42.02, 25.53, 23.67, 22.86, 22.32, 9.31.

Synthesis of organic-inorganic hybrid crosslinker: 6-maleimidohexanoic acid (1 g, 4.74 mmol) and EEDQ (1.7 g, 6.88 mmol) were dissolved in 50 mL anhydrous acetonitrile by vigorously stirring at 80 °C for 15 min, and then a THF solution (50 mL) with DAPO (1.2 g, 1.2 mmol) was slowly added into it. The reaction mixture was refluxing at 80 °C overnight. After that, the solvent was evaporated in vacuo, and the residue was dissolved in acetonitrile (50 mL) and washed with hexane (3 × 100 mL). Precipitation of the concentrated acetonitrile solution into water followed by vacuum filtering afforded organic-inorganic hybrid crosslinker as a brown powder (1.61 g, yield 97%). ^{1}H NMR ($CDCl_3$, 400 MHz, ppm, see Fig. S3a): δ= 8.06 (s, 1H, -$C_6\underline{H}_3$), 7.79 (s, 2H, -$C_6\underline{H}_3$), 7.67 (s, 2H, -N<u>H</u>-CO-CH_2-), 6.67-6.69 (m, 4H, CHs on maleimide groups), 6.43-6.45 (t, 1H, -CH_2-N<u>H</u>-CO-), 3.49-3.55 (m, 4H, -C<u>H</u>$_2$-maleimide), 3.38-3.41 (m, 2H, -C<u>H</u>$_2$-NHCO-), 2.34-2.37 (t, 4H, -C<u>H</u>$_2$-CONH-), 1.81-1.85 (m, 7H, -CH_2-C<u>H</u>-$(CH_3)_2$; 2H, -C<u>H</u>$_2$-CH_2-NHCO-), 1.59-1.71 (m, 12H, -CH_2-(C<u>H</u>$_2$)$_3$-CH_2-), 0.94-0.96 (m, 42H, - CH_2-CH-(C<u>H</u>$_3$)$_2$), 0.62-0.63 (t, 2H, -C<u>H</u>$_2$-CH_2-CH_2-NHCO-), 0.59-0.61 (m, 14H, -C<u>H</u>$_2$-CH-$(CH_3)_2$); ^{13}C NMR ($CDCl_3$, 400 MHz, ppm, see Fig. S3b): δ= 170.72, 169.92, 165.92, 137.99, 134.92, 133.09, 112.56, 112.38, 41.80, 36.48, 36.30, 30.91, 28.34, 27.16, 24.66, 23.74, 22.82, 21.97, 21.67, 21.47, 21.41, 13.10, 8.66.

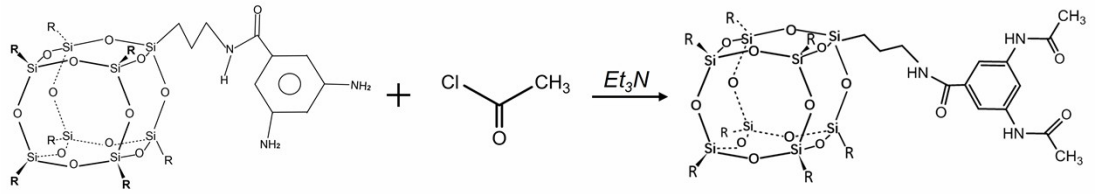

Scheme S2. Schematic representation of synthesis of model Janus nanoparticle.

Synthesis of model Janus nanoparticle: A THF solution (20 mL) with acetyl chloride (0.87g, 11.03 mmol) was slowly added into a THF solution (100 mL) with DAPO (10.55g, 10.46mmol) and triethylamine (1.5 mL) at 0 °C for 30 min. The mixture was stirred at 0 °C for 1 h, and then the mixture was stirred at 25 °C for 5 h. After filtrating, the filtrate was evaporated to remove solution, obtaining an off-white solid. The white solid was dissolved into CH_2Cl_2 and the solution was washed with water, and then dried over Na_2SO_4. After evaporating the solvent under reduced pressure, pure model Janus nanoparticle (11.08 g, 97%) was obtained as a white solid. ^{1}H NMR ($CDCl_3$, 400 MHz, ppm, see Fig. S4a): δ= 8.68 (s, 2H, -N<u>H</u>-CO-CH_3), 8.04 (s, 1H, -$C_6\underline{H}_3$), 7.88 (d, 2H, -$C_6\underline{H}_3$), 6.59 (s, 1H, -CH_2-N<u>H</u>-CO-), 3.38-3.43 (m, 2H, -C<u>H</u>$_2$-NHCO-), 2.15

(s, 6H, -NHCO-C<u>H</u>$_3$), 1.79-1.89 (m, 7H, -CH$_2$-C<u>H</u>-(CH$_3$)$_2$), 1.65-1.73 (m, 2H, -C<u>H</u>$_2$-CH$_2$-NHCO-), 0.94-0.96 (m, 42H, - CH$_2$-CH-(C<u>H</u>$_3$)$_2$), 0.63-0.66 (t, 2H, -C<u>H</u>$_2$-CH$_2$-CH$_2$-NHCO-), 0.59-0.61 (m, 14H, -C<u>H</u>$_2$-CH-(CH$_3$)$_2$); ^{13}C NMR (CDCl3, 400 MHz, ppm, see Fig. S4b):δ= 168.32, 166.52, 138.21, 134.69, 112.67, 41.81, 24.68, 22.81, 21.95, 21.46, 21.40, 8.65.

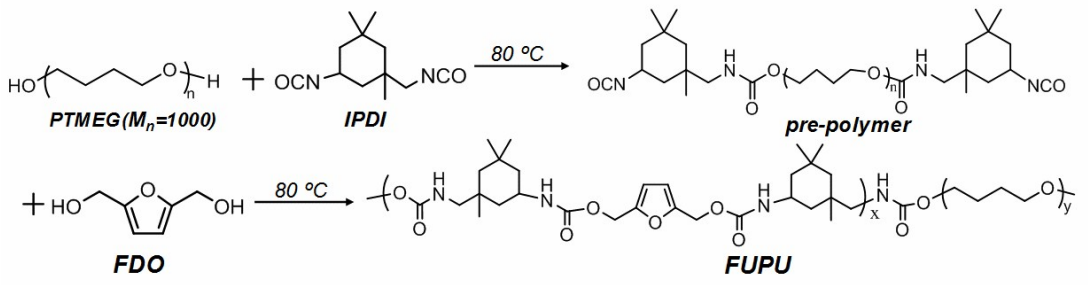

Scheme S3. Schematic representation of synthesis of FUPU.

Synthesis of furan-containing polyurethane (FUPU): According to the previous method,[1] the NCO-terminated prepolymer of polyurethane (pre-polymer) was prepared by the reaction of polytetramethylene ether glycol (PTMEG, Mn= ~1000 g mol^{-1}) and isophorone diisocyanate (IPDI) with a molar ratio of 1: 2 at 80 °C for 8 h. Then, the precursor pre-polymer and the extender 2,5-furandimethanol (FDO) with a molar ratio of 1: 0.95 were reacted at 80 °C in anhydrous dioxane for 12 h, obtaining a liquid-like furan-contained polyurethane (FUPU). ^{1}H NMR spectrums of FUPU are shown in Fig S5 and S6. The molecular weight of FUPU is determined to be 23586 g/mol measured by GPC.

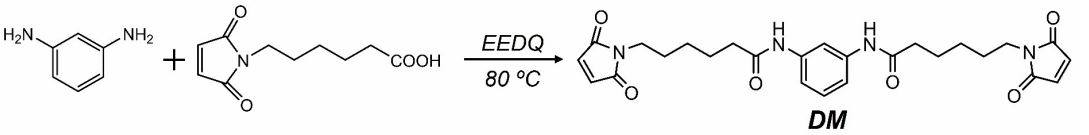

Scheme S4. Schematic representation of synthesis of DM-crosslinker.

Synthesis of DM-crosslinker: 6-maleimidohexanoic acid (1 g, 4.74 mmol) and EEDQ (1.7 g, 6.88 mmol) were dissolved in 50 mL anhydrous acetonitrile by vigorously stirring at 80 °C for 15 min, and then a THF solution (50 mL) with m-phenylenediamine (0.3 g, 2.78 mmol) was slowly added into it. The reaction mixture was refluxing at 80 °C overnight. After that, the solvent was evaporated in vacuo, and the residue was dissolved in acetonitrile (50 mL) and washed with hexane (3 × 100 mL). Precipitation of the concentrated acetonitrile solution into water followed by vacuum filtering afforded DM-crosslinker as an off-white powder (1.29 g, yield 94%). ^{1}H NMR (DMSO-d$_6$, 400 MHz, ppm, see Fig. S6a): δ= 9.82 (s, 2H, -CO-N<u>H</u>-), 7.88 (s, 1H, -C$_6$<u>H</u>$_4$-), 7.23-7.26 (m, 2H, -C$_6$<u>H</u>$_4$-), 7.14-7.18 (m, 1H, -C$_6$<u>H</u>$_4$-), 7.00 (s, 4H, CHs on maleimide groups), 3.39-3.41 (t, 4H, -C<u>H</u>$_2$-maleimide), 2.25-2.28 (t, 4H, -C<u>H</u>$_2$-CONH-), 1.48-1.55 (m, 8H, -NHCO-CH$_2$-C<u>H</u>$_2$-CH$_2$-C<u>H</u>$_2$-CH$_2$-), 1.22-1.24 (m, 4H, -NHCO-CH$_2$-CH$_2$-C<u>H</u>$_2$-CH$_2$-CH$_2$-). ^{13}C NMR (DMSO-d$_6$, 400 MHz, ppm, see Fig. S6b): δ= 171.56, 171.52, 139.99, 134.92, 129.15, 114.34, 110.51, 37.46, 36.61, 28.27, 26.29, 25.11.

Preparation of FUPU nanocomposites: FUPU (3 g, Moles of furan group = 1.821 mmol) was dissolved in dioxane (15 mL). The hybrid crosslinker was added into the solution at different mass ratios (FUPU: hybrid crosslinker = 1:0.25, 1:0.40, and 1:0.55, Table S1) with respect to the FUPU. The mixture was cast into a Teflon mold, and then the mold was put into a vacuum oven at 40 °C under reduced pressure. The temperature was gradually increased to 80 °C with a heating time of 48 h, obtaining a DA-crosslinked FUPU film. The FUPU nanocomposites were designated as POU-*x*, where the "*x*" is the content of hybrid crosslinker. The control sample crosslinked by the DM-crosslinker (DMU) was prepared via the same method. The molar fraction of the DM-crosslinker in DMU is equal to that of the hybrid crosslinker in POU-40. The formulations of DMU and POU-x are listed in Table S1.

Instruments and Methods:
Nuclear Magnetic Resonance (NMR): ^{1}H NMR and ^{13}C NMR spectra were measured on an Avance III HD 400 MHz spectrometer (Bruker). $CDCl_3$ and DMSO-d_6 were used as the solvents.

Gel permeation chromatography (GPC): The molecular weight was measured by gel permeation chromatography with THF as the eluent.

UV-vis spectroscopy: The model Janus nanoparticles were firstly dissolved in $CHCl_3$/hexane (v_1/v_2= 1/99) at different concentration, and then the UV absorption spectrum for the solution was conducted on a SHIMADZU UV-2600 ultraviolet spectrophotometer. The spectra scanned from 400 nm to 200 nm with a medium scanning mode. The UV-vis transmitted spectrum of the FUPU nanocomposites was conducted on the same machine using an integrating sphere attachment. The spectra scanned from 800 nm to 300 nm with a medium scanning mode.

Fourier transform infrared spectroscopy (FTIR): FTIR spectra were recorded on a Thermo Scientific Nicolet iS50 FTIR equipped with a heating cell. At first, the mixture of hybrid crosslinker and FUPU were dissolved into dioxane (1 wt %), and then we dispensed 2-3 drops of the dilute solution of mixture onto KBr pellet. Finally, the pellet was put into the heating cell at a constant temperature of 80 °C for time-dependent FTIR measurement. In order to perform a temperature-dependent FTIR measurement for POU-*x*, the KBR pellet coated by the mixture of organic-inorganic hybrid crosslinkers and FUPU was put into oven at 80 °C for 12 h first. After the curing, the pellet was put into the heating cell upon heating from 20 °C to 100 °C at a rate of 1 °C/min for the temperature-dependent FTIR measurement.

Dynamic Light Scattering (DLS): DLS measurements were carried out by a wide angle laser scattering instrument (BI-200SM, Brookhaven) equipped with a cuvette rotation/translation unit (CRTU) and a He-Ne laser (22 mW, wavelength λ of 632.8 nm) to study the mean diameter of RHP.

Transmission electron microscopy (TEM): TEM tests were performed on a FEC Tecnai G^2 F20 S-TWIN (the acceleration voltage was 200 kV) electron microscope. The model Janus nanoparticles were dissolved into $CHCl_3$/hexane (*v*/*v*=1/99) with a concentration of 2×10^{-5} M, and then the solution was dripped on a copper mesh equipped a carbon film for TEM

measurement. The FUPU nanocomposites were frozen to -100 °C, and then they were cut into ultrathin sections with thickness of about 80 nm using a Leica EMUC6/FC6 ultrathin slicer. The sections of the FUPU nanocomposites were placed in a copper grid for TEM measurement. The ultrathin section of DMU was prepared via the same method. Before the TEM measurement, the grid containing the DMU sections was exposed to 0.5% ruthenium tetroxide (RuO_4) in solution by affixing the grids with tape in a glass Petri dish and suspending them over a droplet of the RuO_4 for 2 h.

X-ray Diffraction (XRD): XRD analysis was conducted on a PhilipsX'Pert PRO diffractometer (Holland) with Cu Kα radiation (λ = 0.154 nm) at room temperature. The model Janus nanoparticles were dissolved in $CHCl_3$/hexane (*v*/*v*=1/99). After the evaporation of solvent, the residual solids composed of large amounts of supramolecular nanosheets were measured by XRD.

Small-Angle X-ray Scattering (SAXS): SAXS experiments were performed on a D8 Discover (Bruker) equipped with a 2D VANTEC 500 detector. The working voltage and current for the X-ray tube were 40 kV and 40 mA, respectively. The wavelength of the X-ray is 0.154 nm. Temperature-dependent SAXS measurements were performed on the same machine, and the samples were placed into a heating stage with a heating rate of 5 ºC/min.

Differential scanning calorimeter (DSC): DSC tests were performed on a TA Instruments DSCQ2000 with the mass of all samples ranging from 3 mg to 8 mg. The FUPU nanocomposites were heated from -50 °C to 100 °C at a heating rate of 10 °C/min and then cooling to -50 °C at 10 °C/min. The heating and cooling processes were performed two times.

Tensile test: Tensile experiments were performed on an Instron 5967 tensile tester. Uniaxial tensile measurements were carried out in air at room temperature with a strain rate of 100 mm/min. The FUPU nanocomposites were cut into the dumbbell shaped samples by a normalized cutter, where the length, width and thickness of the central part were 20 mm, 4 mm and 0.5-1 mm, respectively.

Water absorption measurement: Wafer-like samples were immersed in deionized water, where the thickness and diameter of the samples were 1 mm and 10 mm, respectively. Then, the gaining weight of the swelled samples were recorded periodically.

Humidity resistance measurement: The FUPU nanocomposites were put into a closed container with a relative humidity (RH) of 97%, where the humidity environment was provided by the saturated aqueous solution of K_2SO_4.[2] After 72 hours, the FUPU nanocomposites were taken out from the container, and then the mechanical properties of the FUPU nanocomposites were measured by tensile test.

Contact angle: Water contact angles (WCA) of the FUPU nanocomposites were measured using a Rame-Hart 260 F4 standard goniometer at room temperature. A drop of water was placed onto the surface of the polymer film, and then the contact angles were measured within

10 s. Three tests were performed at different positions on the surface of polymer film for each sample.

Gas Permeability Measurement: The gas permeability test was performed using a VAC-V1 gas permeability tester (Labthink Instrument Co., China) at 40 °C and 50% relative humidity (RH) according to ISO15105-1:2007, based on the pressure difference method. A wafer-like sample with a diameter of 50 mm was placed into the gas permeation cell to form a sealed barrier between a lower chamber with high vacuum pressure and a upper chamber containing air at 0.1 MPa. The air permeability coefficient (P_{air}) was determined by tracing the pressure variations with time in the lower chamber. Three independent specimens were tested for each sample for obtaining reliable results.

Optical microscopy (OM): The on-line tracing for the recovery of crack was performed on an optical microscope (MDA2000, Future Optics) equiped with a heating stage. The scratched samples were made by a razor blade and placed into the heating stage at 110 °C; then the photographs of the samples were taken using a digital camera Olympus DP-27.

Theoretical calculation

Molar fraction of furan groups (c_{fu}): The content of furan group in per gram of FUPU ($\boldsymbol{c_{fu}}$) can be calculated by following equation:

$$c_{fu} = \frac{n_{FDO}}{m_{PTMEG} + m_{IPDI} + m_{FDO}}$$

where the n_{FDO} is the moles of consumed FDO, the m_{PTMEG} is the mass of consumed PTMEG, the m_{IPDI} is the mass of consumed IPDI and the m_{FDO} is the mass of consumed FDO in the synthesis of FUPU. By calculation, the value of c_{fu} is 0.607 mmol/g.

Toughness (U_T): The toughness (U_T) was calculated by the integrated area below the stress-strain curves as illustrated by following equation:

$$U_T = \int_0^{\sigma_b} \sigma d\varepsilon$$

where the σ stands for the stress, ε stands for the strain and σ_b is the fracture stress.

Relative mass uptake (M): To reduce any systematic error involved in water absorption measurement, the relative mass uptake *M(t)* determined gravimetrically with exposure times is calculated by following equation:[3]

$$M(t) = \frac{W(t) - W(0)}{W(0)}$$

where *W(t)* is the weight of a specimen after an exposure time *t* and *W(0)* is calculated theoretically by determining the intercept of the linear fitting of *W(t)* against $t^{1/2}$ at t=0.

Diffusion coefficient of water (D): The diffusion coefficient of water (*D*) is determined by following equation:[3]

$$\frac{4M(\infty)}{h\sqrt{\pi}}\sqrt{D} = \frac{M_2 - M_1}{\sqrt{t_2} - \sqrt{t_1}}$$

where *h* is the thickness of the samples and *M(∞)* is the mass uptake at the saturation point of the absorption.

Self-healing efficiency: Healing efficiency (*η*) is calculated according to the following equation:

$$\eta = \frac{\sigma_{heal}}{\sigma_{pri}} \times 100\%$$

where σ_{heal} is the tensile strength of the healing samples, and σ_{pri} is the tensile strength for the pristine samples.

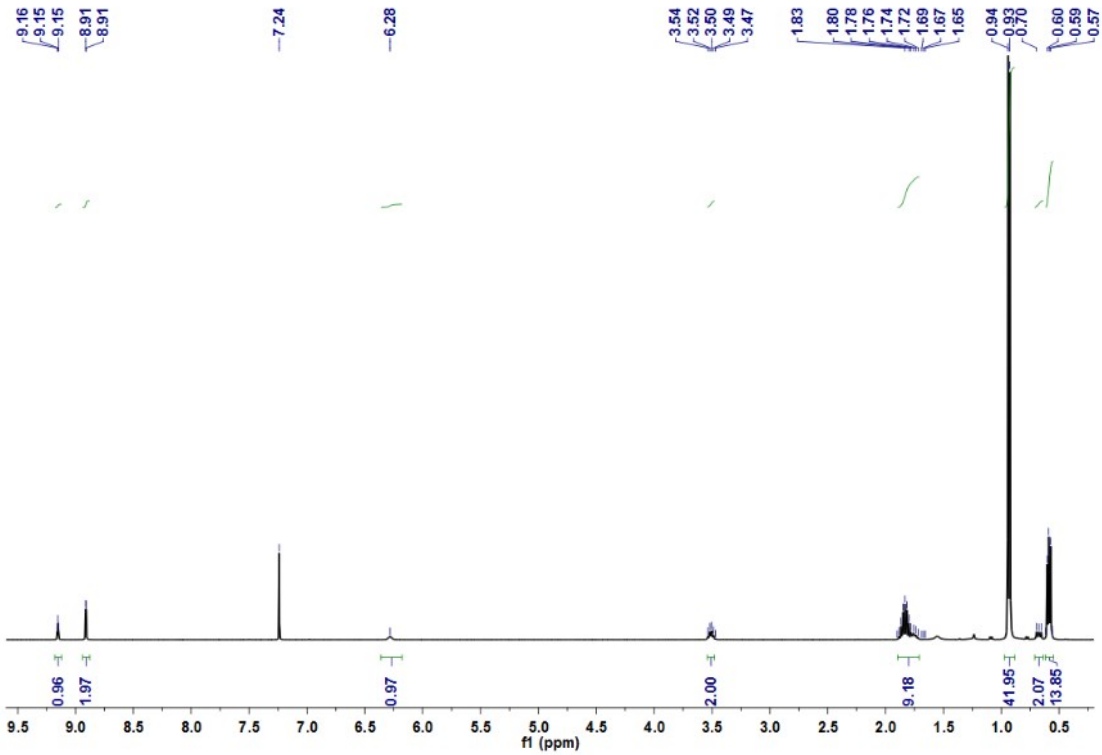

Figure S1a. ^{1}H NMR spectrum of DNPO ($CDCl_3$).

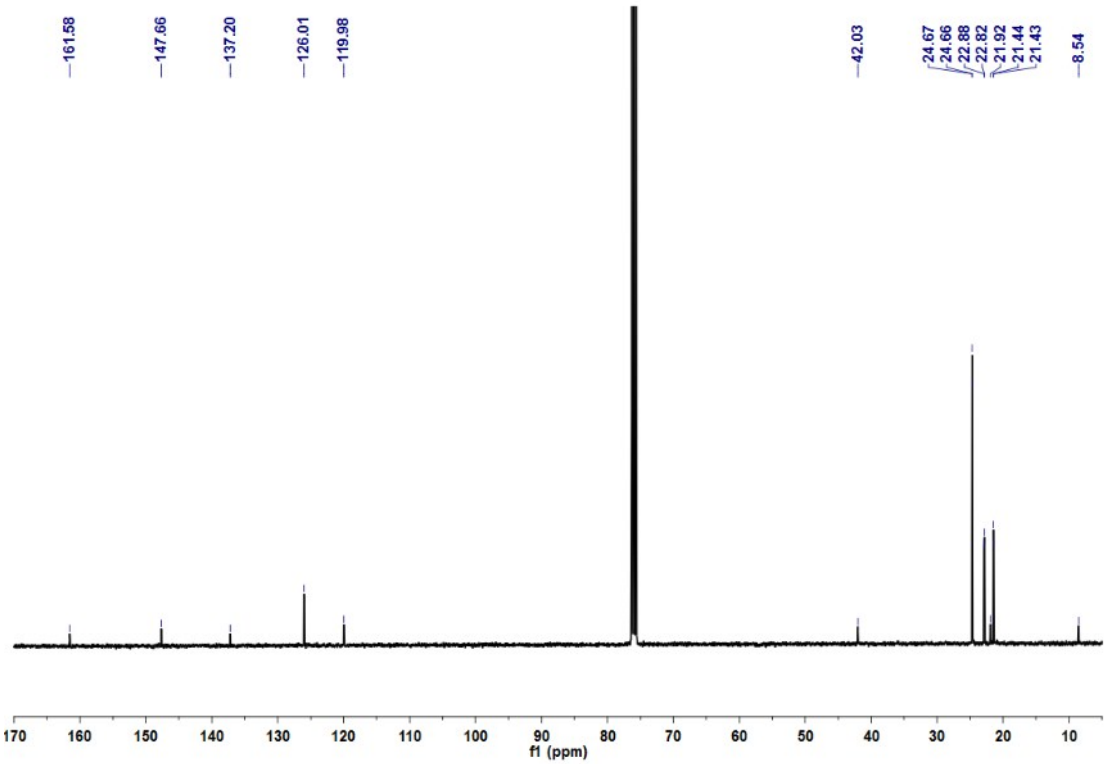

Figure S1b. ^{13}C NMR spectrum of DNPO ($CDCl_3$).

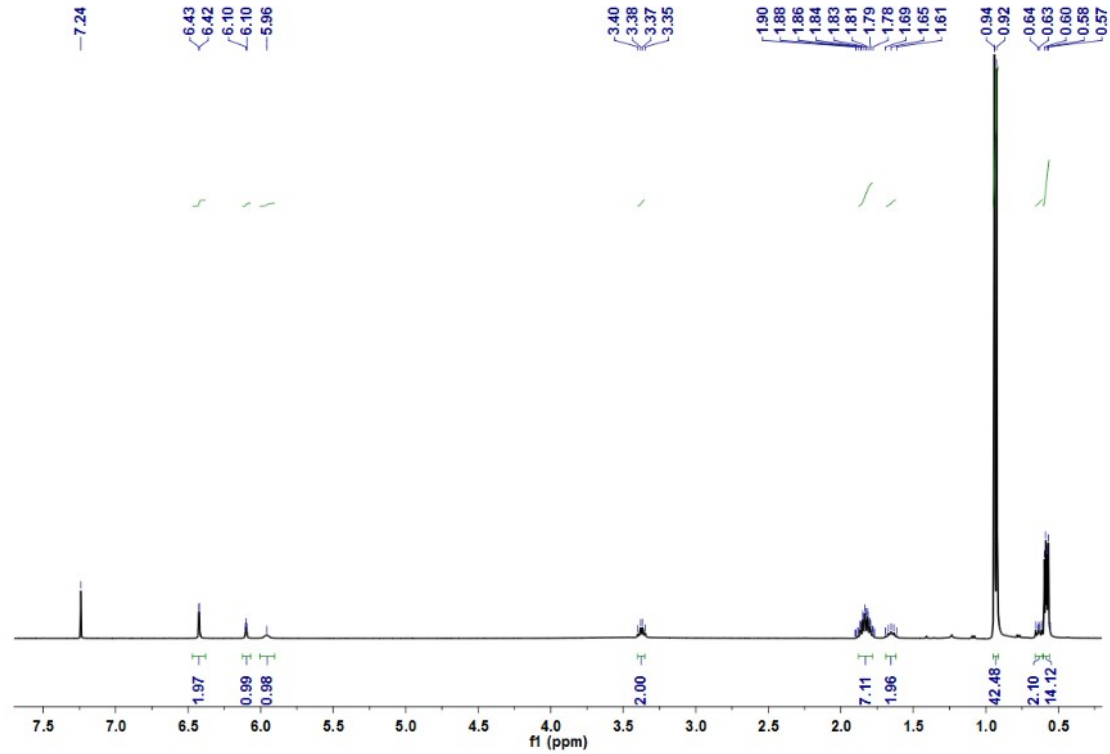

Figure S2a. ^{1}H NMR spectrum of DAPO ($CDCl_3$).

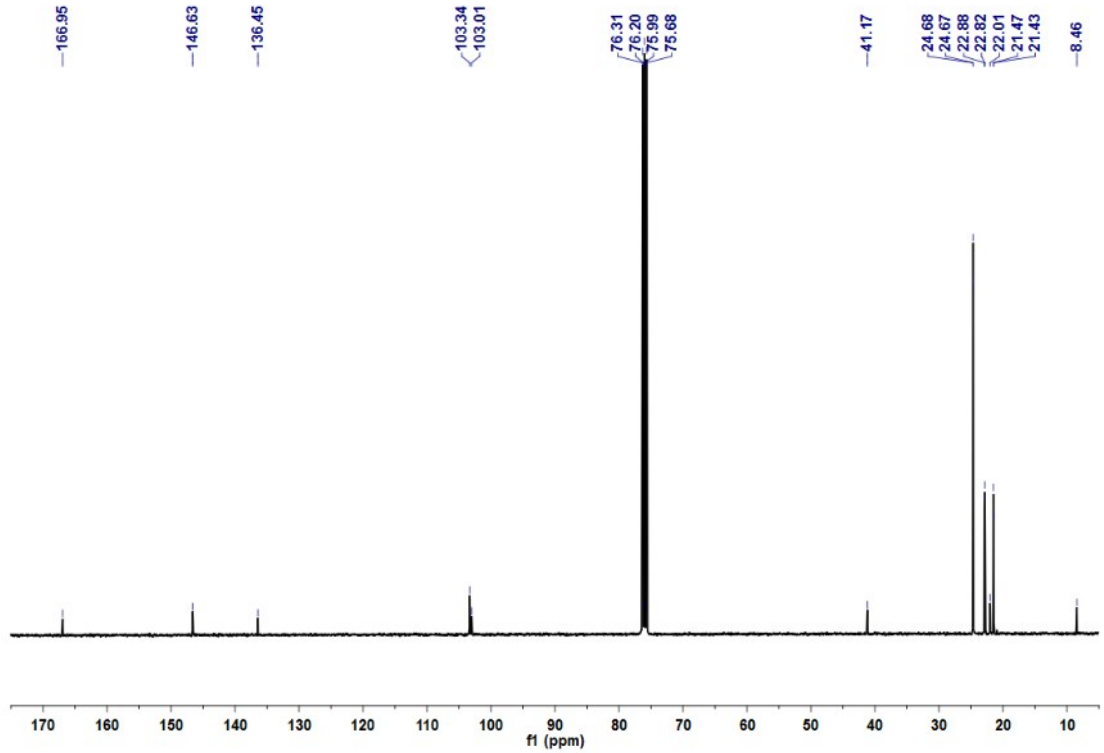

Figure S2b. ^{13}C NMR spectrum of DAPO ($CDCl_3$).

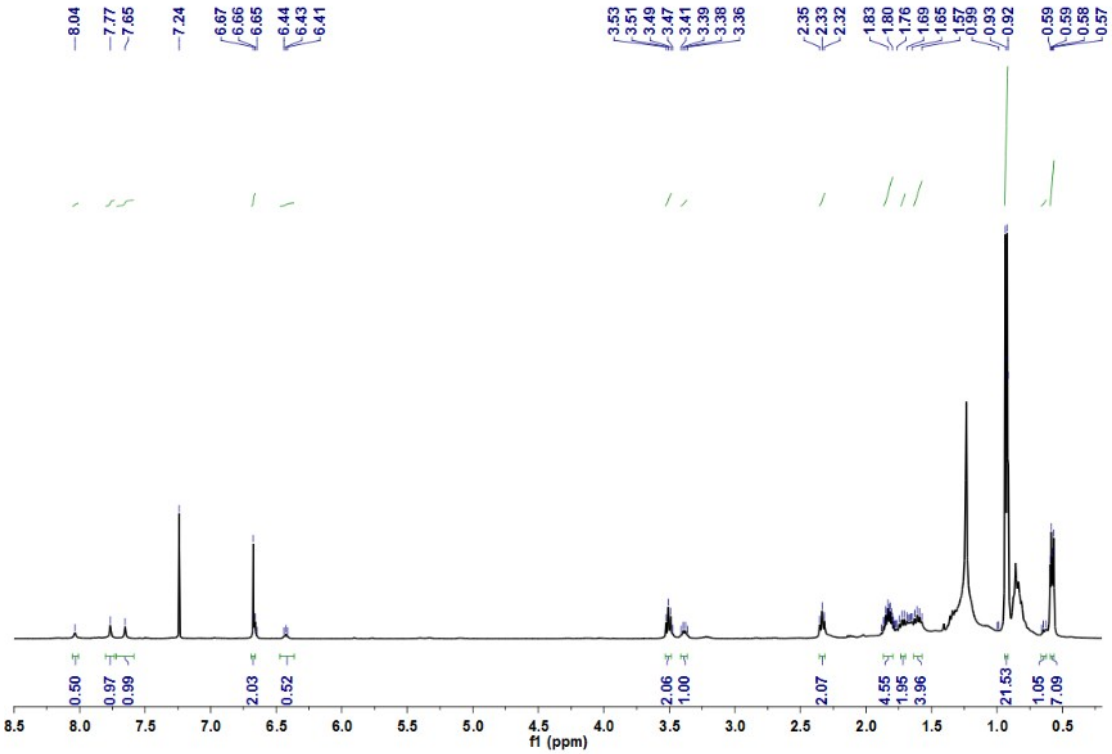

Figure S3a. ^{1}H NMR spectrum of organic-inorganic hybrid crosslinker ($CDCl_3$).

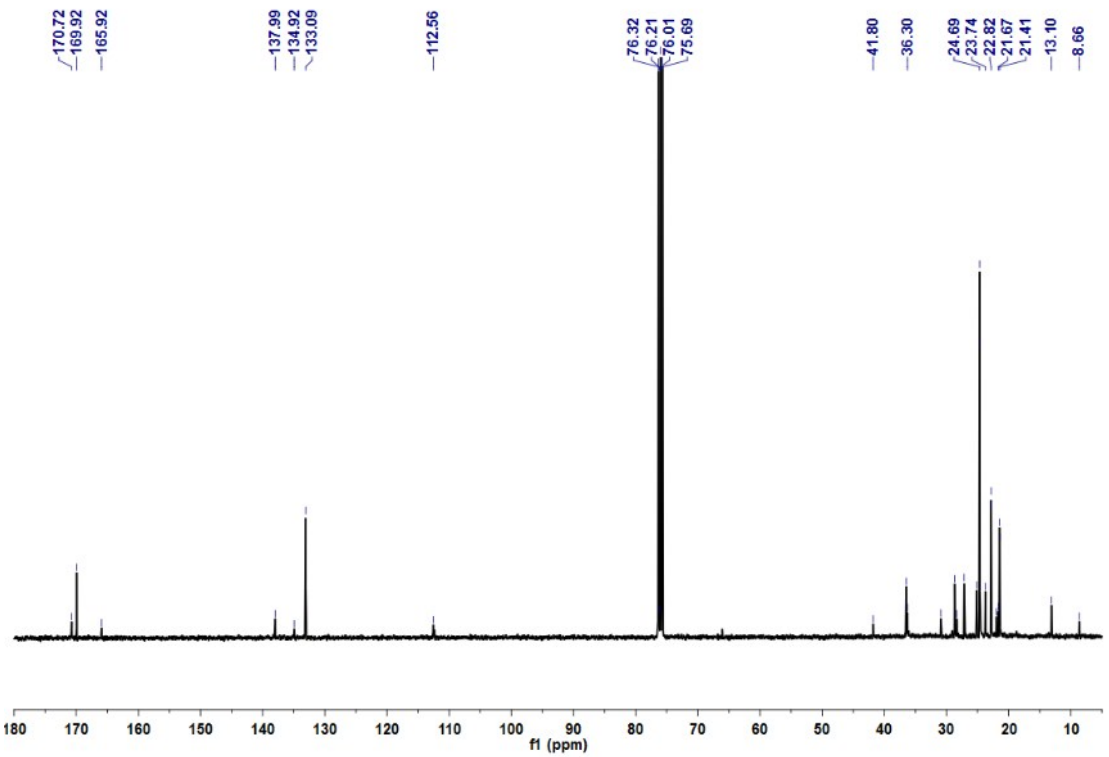

Figure S3b. ^{13}C NMR spectrum of organic-inorganic hybrid crosslinker ($CDCl_3$).

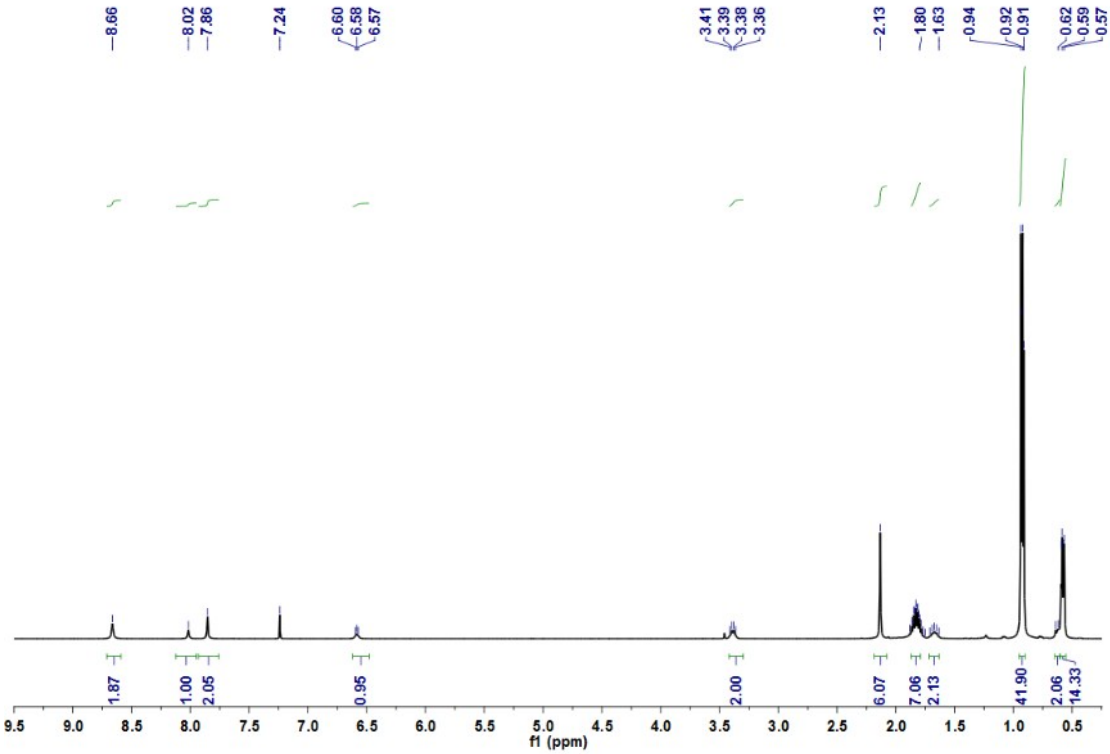

Figure S4a. ^{1}H NMR spectrum of model Janus nanoparticle ($CDCl_3$).

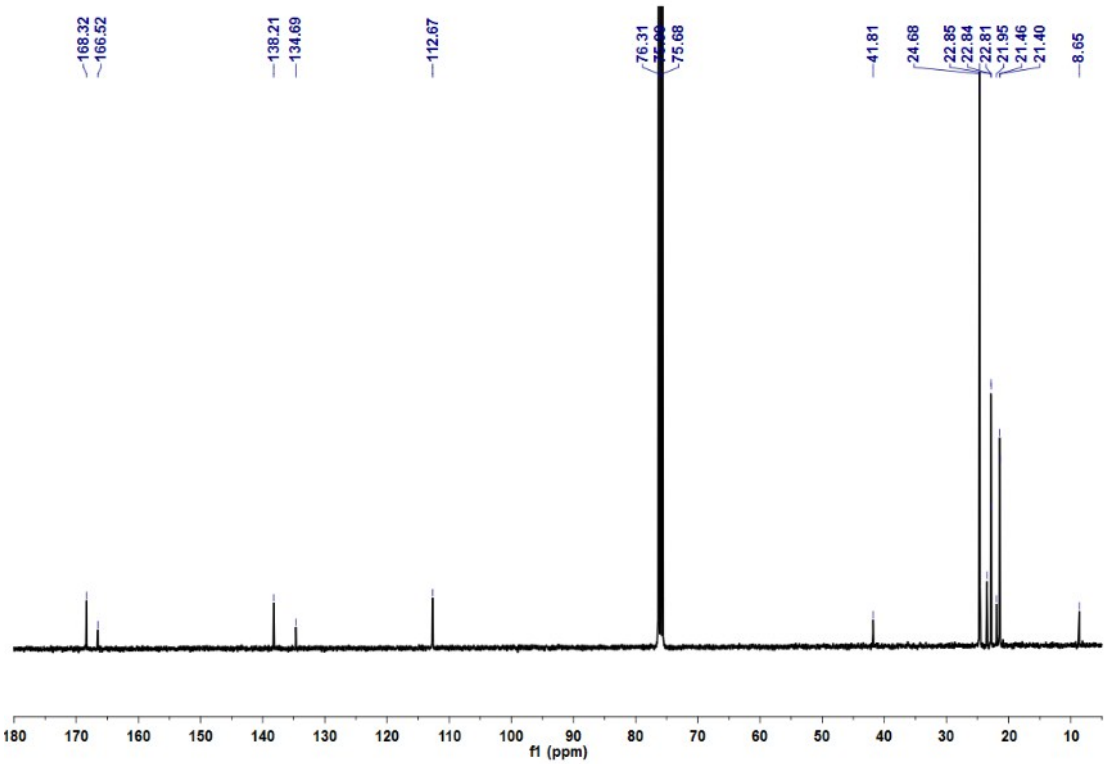

Figure S4b. ^{13}C NMR spectrum of model Janus nanoparticle ($CDCl_3$).

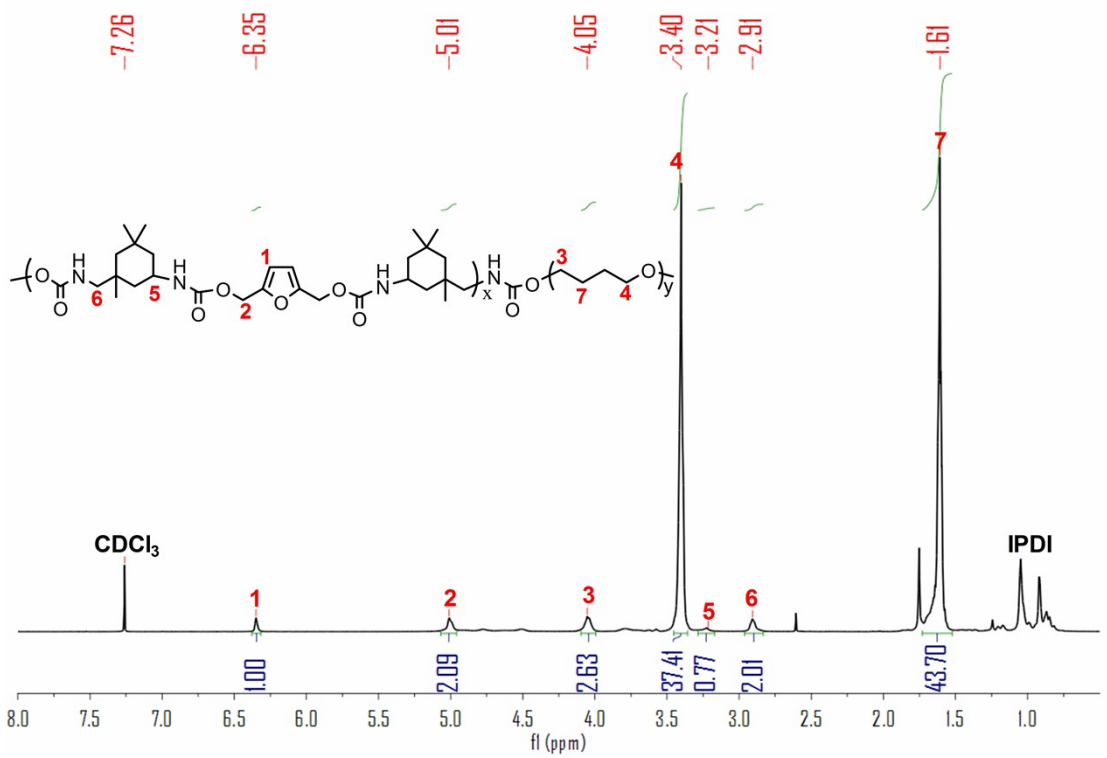

Figure S5. ^{1}H NMR spectrum of FUPU ($CDCl_3$).

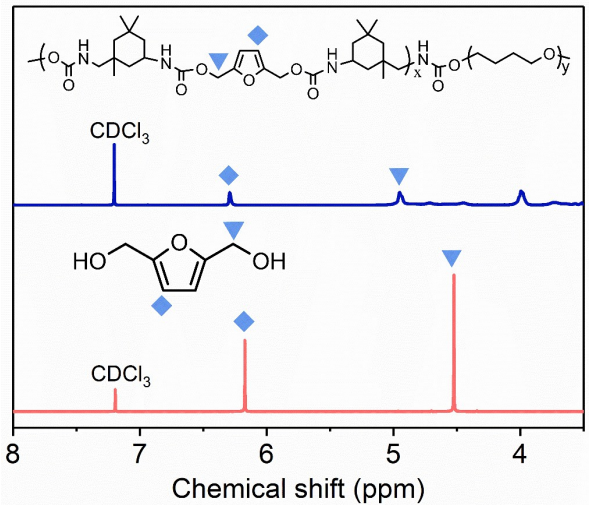

Figure S6. ^{1}H NMR spectrums ($CDCl_3$) of FDO (red) and FUPU (blue). Due to the generation of carbamate groups (-NH-COO-) which possess stronger electronegativity than hydroxy groups, the signal of protons of the -CH_2- in FDO at 4.59 ppm completely shifts to 5.01 ppm, and the signal of proton of the furan ring shifts from 6.24 ppm to 6.35 ppm, exhibiting the high efficiency of the chain extension reaction between the pre-polymer and FDO.

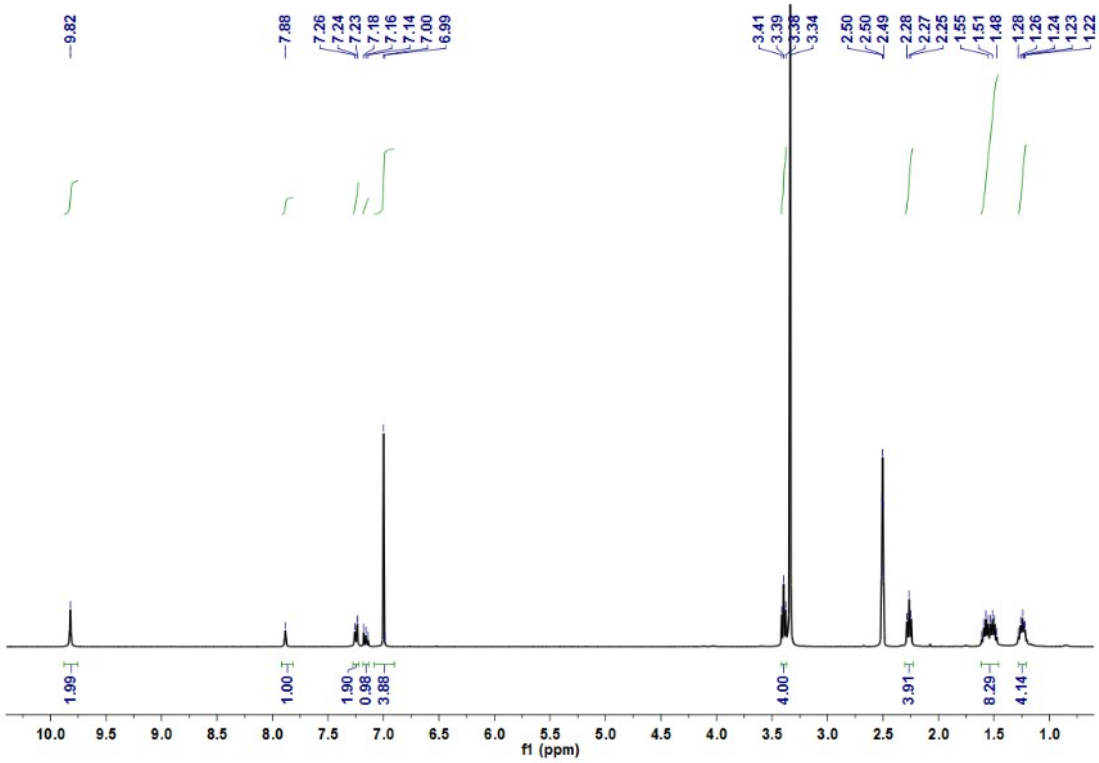

Figure S7a. ^{1}H NMR spectrum of DM (DMSO-d_6).

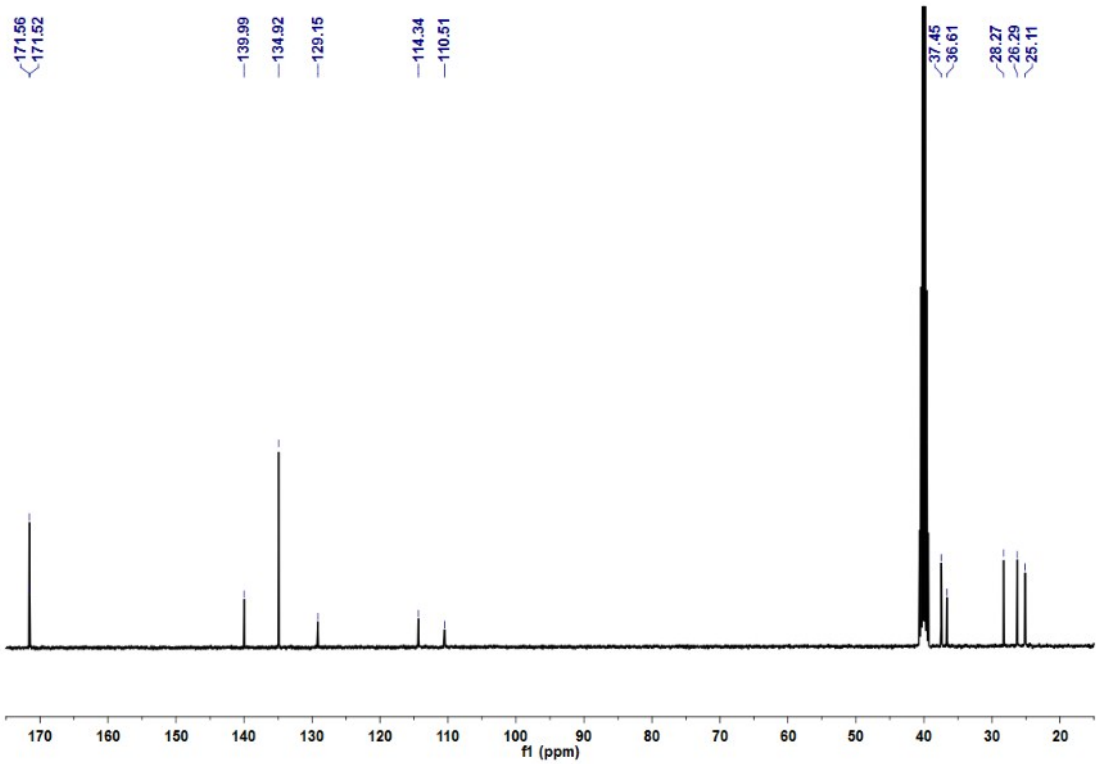

Figure S7b. ^{13}C NMR spectrum of DM (DMSO-d_6).

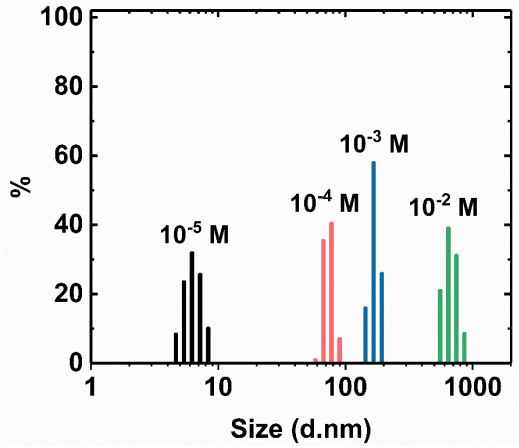

Figure S8. Concentration-dependent DLS analysis for the nanosheets assembled in $CHCl_3$/hexane (*v*/*v* = 1/99).

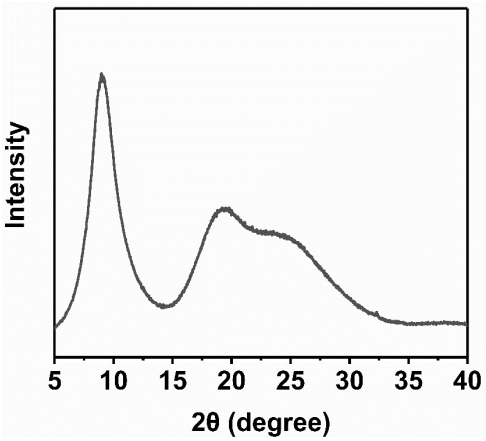

Figure S9. XRD curve for the supramolecular nanosheets assembled in solution.

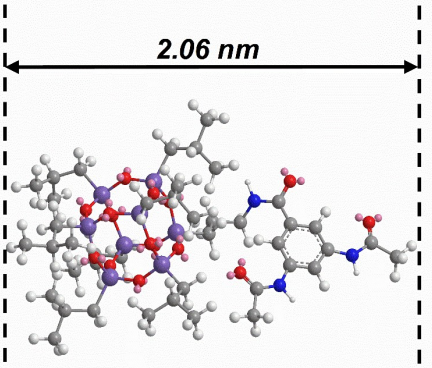

Figure S10. Molecular model of the model Janus nanoparticle with energy minimization, and the calculated axial length of the model Janus nanoparticle with a minimized free energy of 13.11 kcal/mol is 2.06 nm via molecular simulation.

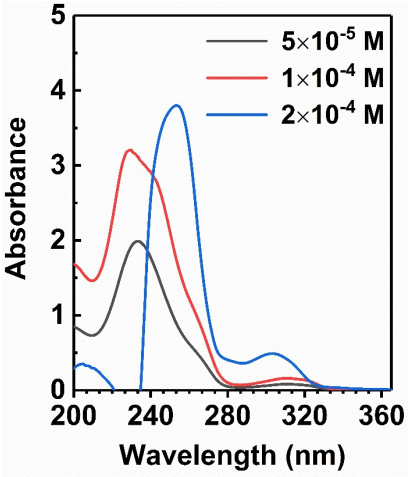

Figure S11. Concentration-dependent UV-vis spectrum of the model Janus nanoparticles in $CHCl_3$/hexane (*v*/*v* = 1/99).

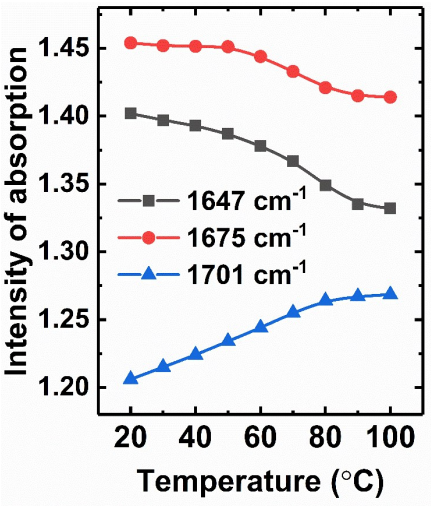

Figure S12. The intensity of absorption bands at 1701 cm^{-1}, 1675 cm^{-1} and 1647 cm^{-1} in the temperature-dependent FTIR spectrum of the supramolecular nanosheets as a function of temperature. The absorption band at lower wavenumber (1647 cm^{-1}) can be assigned to the stretching vibration of the carbonyls of (-C_6H_3-CO-NH-), while the absorption band at 1675 cm^{-1}

can be ascribed to the stretching vibrations of the carbonyls of (-C_6H_3-NH-CO-), as the conjugative effect between the aromatic core and the carbonyl of (-C_6H_3-CO-NH-) can reduce the absorption frequency of carbonyl.[4]

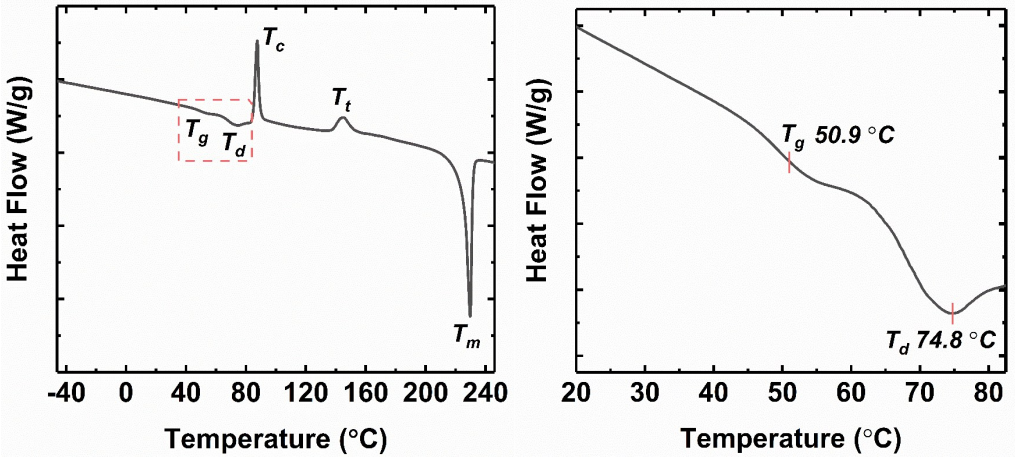

Figure S13. DSC thermogram for the supramolecular nanosheets assembled in solution at a heating rate of 10 ºC/min (left side), and its amplified curve between 20 ºC and 85 ºC (right side). The step-like endothermic peak at 51 ºC can be ascribed to the glass transition temperature (***T_g***) of supramolecular nanosheets. The second transition temperature at 75 ºC is approximate to the dissociation temperature of the hydrogen bonds of the 3-fold amides measured by temperature-dependent FTIR, and thus this structural transition can be assigned to the dissociation of the stacked BTA moieties upon heating. The sharp exothermic peak at 87.5 ºC represents the crystallization of the supramolecular nanosheets, and another exothermic peak at 144.6 ºC can be ascribed to the phase transition temperature of crystal. The sharp endothermic peak at 229.8 ºC is the melting point of crystal. These results indicate that the supramolecular nanosheets are firmly locked by the stacked BTA moieties, enabling their high stability at ambient condition.

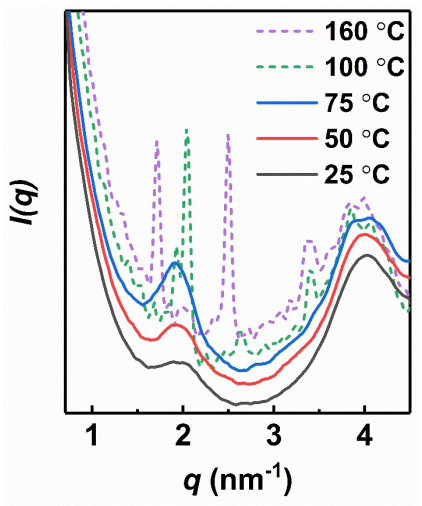

Figure S14. Temperature-dependent 1D SAXS curves of the supramolecular nanosheets assembled in solution. After the temperature reaches above the T_g of the supramolecular nanosheets, the peak at q_1 becomes more and more sharp with the rising of temperature, indicating that the supramolecular nanosheets become unstable upon heating. It is because

that the Janus nanoparticles have to adopt more ordering packing for maintaining the amorphous 2D nanostructure as the decrased stability of the supramolecular nanosheets. The emergence of several sharp peaks at 100 ºC confirms the crystallization of the model Janus nanoparticles upon heating. When the temperature reaches 160 ºC, the positions of the crystalline peaks shift distinctly, reflecting the phase transition of the crystal formed by the model Janus nanoparticles.

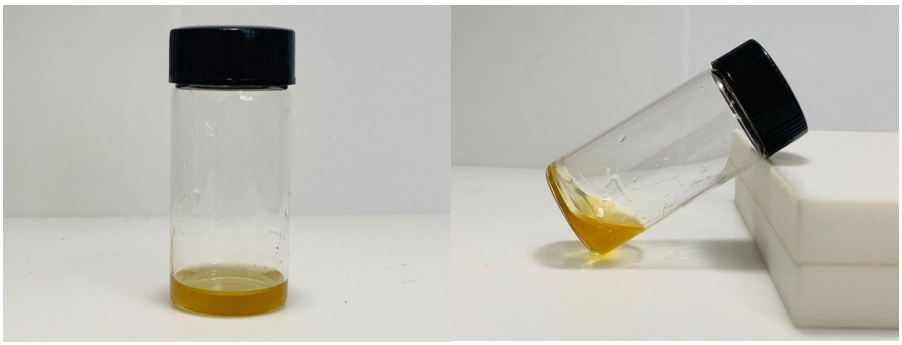

Figure S15. Images for the liquid-like FUPU.

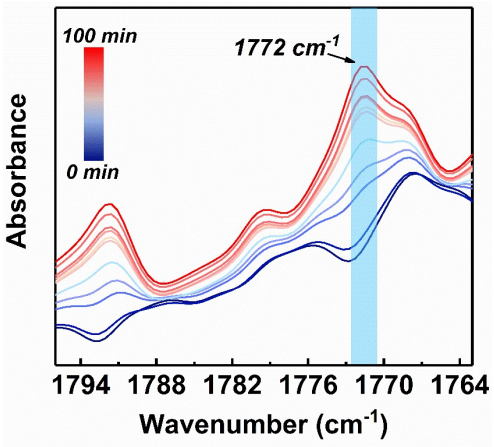

Figure S16. Time-dependent FTIR spectra (1780-1760 cm^{-1}) for the DA reaction between the FUPU and hybrid crosslinker at 80 ºC.

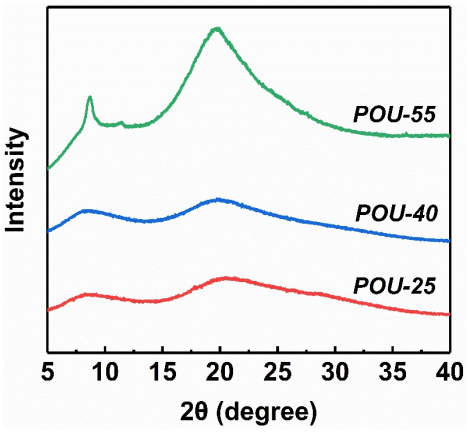

Figure S17. XRD curves of the FUPU nanocomposites. The sharp peak at 2Θ= 8.98º on the XRD curve of POU-55 indicates that the nanosheets in POU-55 are crystalline, while the emergence of the diffuse-like peaks on the XRD curves of POU-25 and POU-40 reveal that both the nano-aggregations in POU-25 and the nanosheets in POU-40 are amorphous.

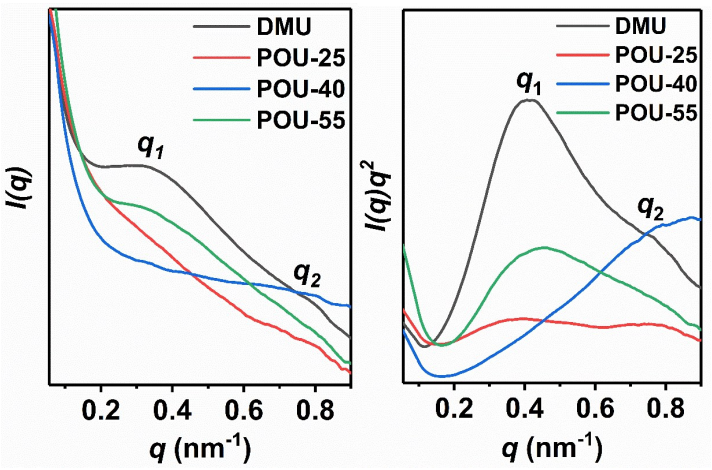

Figure S18. 1D SAXS curves of the FUPU nanocomposites (left side), and their *Lorentz* corrected SAXS plots (right side). The first diffuse-like peak at 0.42 nm^{-1} on the SAXS curve of DMU demonstrates the aggregations formed by the DM-crosslinker are phase-separated from the FUPU with long-range order, and the interdomain spacing (d_1) is 15.3 nm (calculated via $d_1 = 2\pi/q$). The second diffuse-like peak at 0.77 nm^{-1} can be assigned to the size of the hard domains formed by the DM-crosslinker, and the feature size of the hard domains is 8.2 nm. The diffuse-like peak at around 0.4 nm^{-1} on the SAXS curve of POU-55 can be ascribed to the interdomain spacing of the crystalline nanosheets in POU-55. There is no peak on the SAXS curve of POU-40 in the range of q < 1 nm^{-1}, indicating that the amorphous nanosheets are randomly distributed in the POU-40, which agrees well with the TEM results. In addition, no peak appears at around 0.77 nm^{-1} on both the SAXS curves of POU-40 and POU-55, as the peak assigned to the thickness of nanosheets appears at around 1.2 nm^{-1}.

.

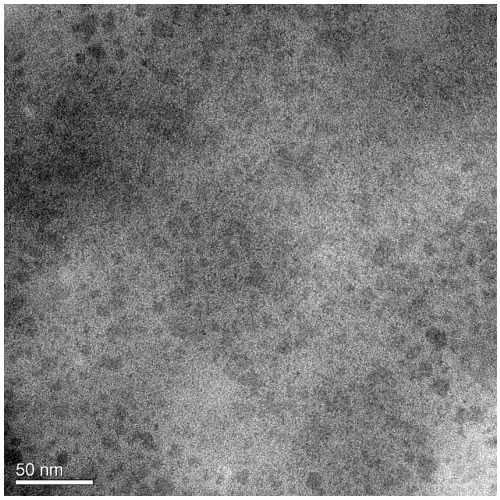

Figure S19. TEM image with staining for the cross-section of DMU. The dark domains with an average size of ~ 8 nm represent the hard domains formed by the DM-crosslinker.

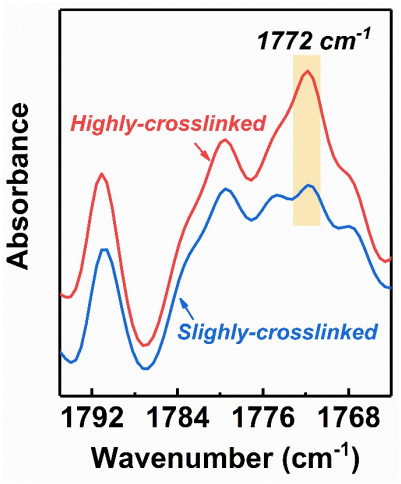

Figure S20. FTIR spectrums of the non-heat-treated POU-40 (blue) and heat-treated POU-40 (red).

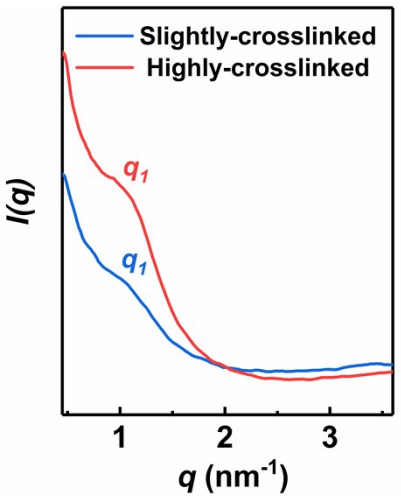

Figure S21. 1D SAXS curves of the slightly-crosslinked POU-40 and the highly-crosslinked POU-40.

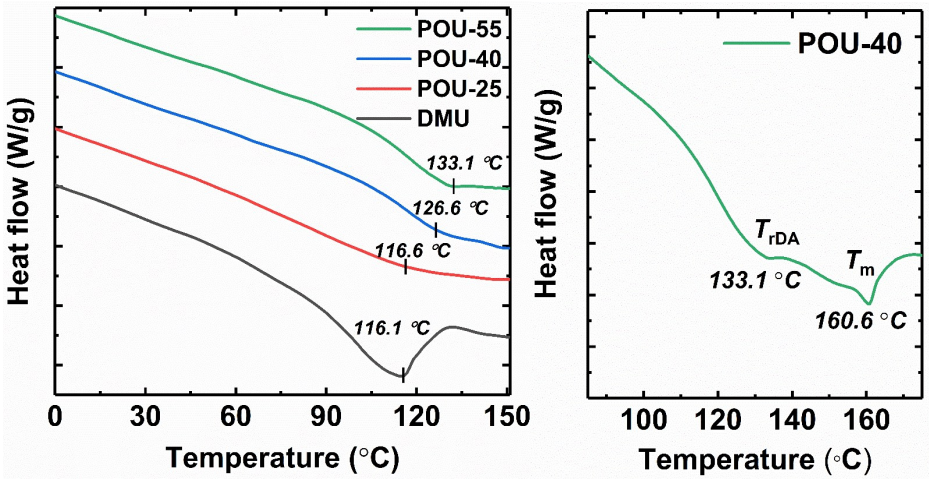

Figure S22. DSC thermograms for the FUPU nanocomposites at a heating rate of 10 ºC/min (left side) and the amplified DSC thermogram in high temperature region for POU-55 (right side). The broad endothermic peaks at 116.1 ºC, 116.6 ºC, 126.6 ºC and 133.1 ºC for DMU,

POU-25, POU-40 and POU-55, respectively, can be assigned to the *r*-DA temperature ($T_{r\text{-}DA}$).[5]

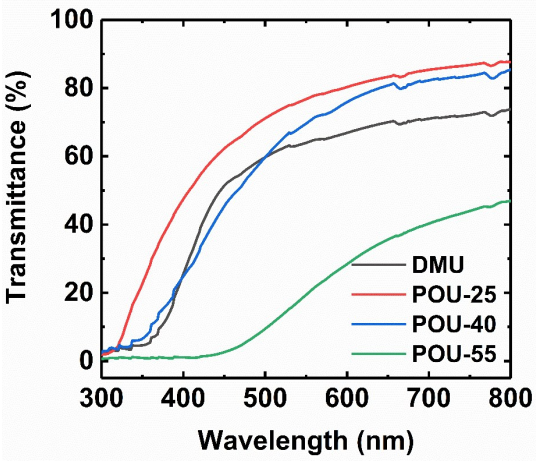

Figure S23. UV-vis spectrums of the FUPU composites.

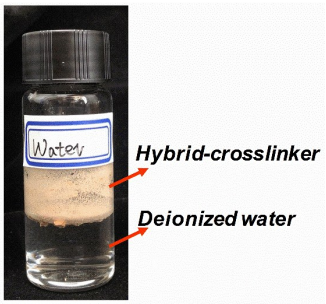

Figure S24. Image of the organic-inorganic hybrid crosslinker mixed with water. The image shows that the hybrid crosslinker floats on the water surface and bottle wall, and the deionized water is totally unable to wet the hybrid crosslinker, demonstrating that the hybrid crosslinker is extremely hydrophobic.

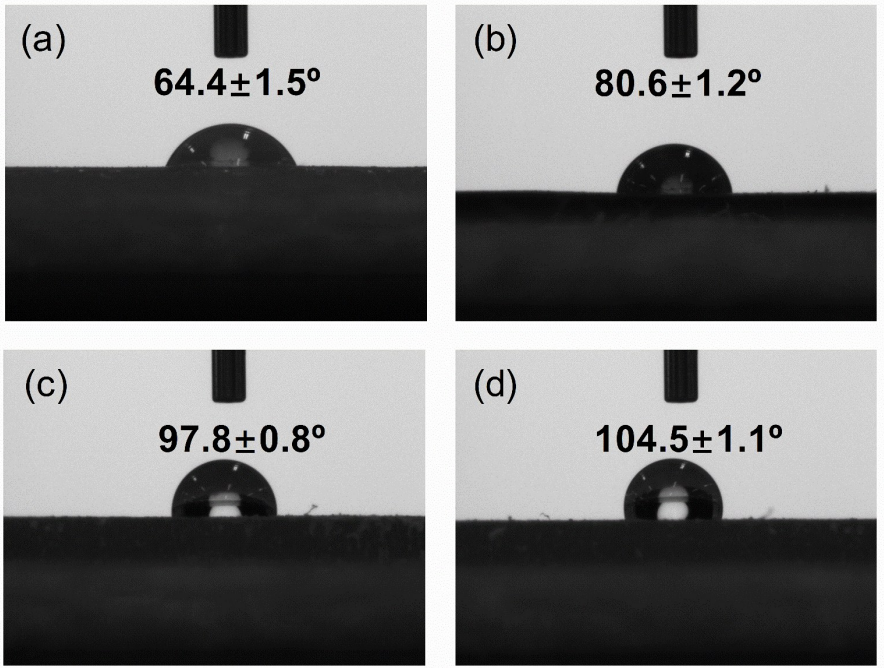

Figure S25. Images of water droplets and water contact angles on a) DMU, b) POU-25, C) POU-40 and d) POU-55.

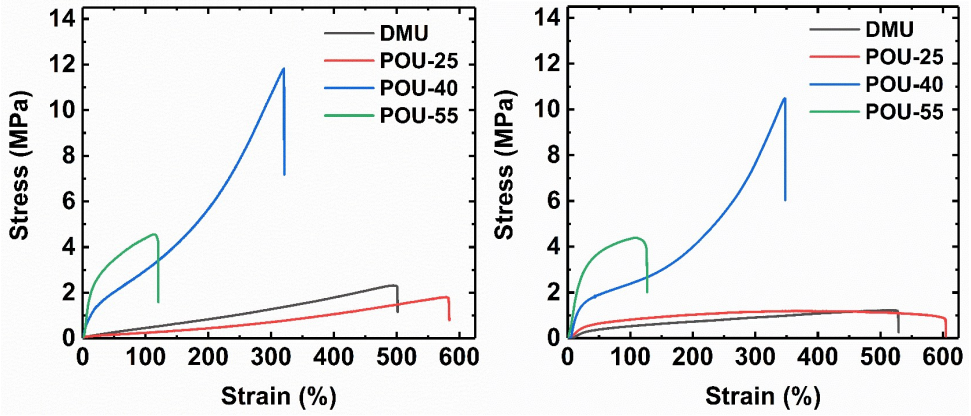

Figure S26. Stress-strain curves of the FUPU nanocomposites, which are placed into high humidity environment (97% RH) for 72 hours (left side) and immersed in water at room temperature for 72 hours (right side).

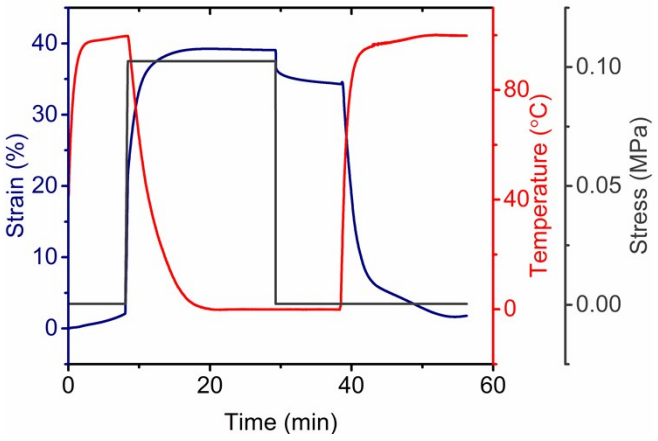

Figure S27. Shape memory property of POU-40.

Table S1. Formulations of DMU and POU-x composites.

Samples	FUPU:Hybrid crosslinker (Mass ratio)	FUPU:DM (Mass ratio)	Maleimide : Furan (molar ratio)	*i-butyl* POSS moieties mass fraction (%)
POU-25	1:0.25	/	0.7:1	12.4
POU-40	1:0.40	/	1:1	17.7
POU-55	1:0.55	/	1.3:1	22.1
DMU	/	1:0.15	1:1	/

Table S2. Mechanical properties of DMU and POU-x composites.

Sample	Tensile strength (MPa)	Elongation at break (%)	Young's modulus (MPa)	Toughness (MJ/m^3)
DMU	5.21±0.32	475±11	1.97±0.11	10.81±0.7
POU-25	3.42±0.23	574±15	1.42±0.09	9.64±0.9
POU-40	12.36±0.43	332±12	8.87±0.5	17.75±0.7
POU-55	4.73±0.25	116±9	14.54±0.6	4.03±0.3

Table S3. Retention rate of tensile strength (R_t) of the FUPU nanocomposites in high humidity and water environment.

Sample	DMU	POU-25	POU-40	POU-55
R_t in humidity environment (%)	44.3	53.5	95.9	97.1
R_t in water environment (%)	24.2	34.8	85.1	93.2

Supplemental References

[1] F. Daihua, P. Wuli, W. Zhanhua, L. Xili, S. Shaojie, Y. Changjiang, X. Hesheng, *J. Mater. Chem. A* **2018**, 6, 18154.

[2] C. Yang, H. Zhang, Y. D. Liu, Z. L. Yu, X. D. Wei, Y. F. Hu, *Adv. Sci.* **2018**, 5, 1801070.

[3] L. R. G. Treloar, *Proc. R. Soc. London* **1950**, 200, 176.

[4] S. Cantekin, T. F. A. de Greef, A. R. A. Palmans, *Chem. Soc. Rev.* **2012**, 41, 6125.

[5] B. P. Kumar, M. Prantik, S. N. K., *Macromolecules* **2018**, 51, 4770.